



# Effects of textured surfaces on the properties of hydrodynamic bearing

Yusheng Niu<sup>1</sup> · Xiuqing Hao<sup>1,2</sup> · Annan Xia<sup>1</sup> · Li Wang<sup>2</sup> · Qiankai Liu<sup>1</sup> · Liang Li<sup>1</sup> · Ning He<sup>1</sup>

Received: 26 May 2021 / Accepted: 6 September 2021 / Published online: 18 September 2021  
© The Author(s), under exclusive licence to Springer-Verlag London Ltd., part of Springer Nature 2021

## Abstract

Hydrodynamic bearing is becoming an indispensable component of high-accuracy devices such as high-speed machine tools. Recently, the study of textured surface bearing has become one of the highly researched topics. Among the different types of surface texture, partially textured bearing shows outstanding performances on anti-vibration. However, most of the research focuses on the theoretical models of partial texture. In this paper, several bearings with no texture, full texture and partial texture are fabricated for stability and stiffness tests. The result shows that the partially textured bearings with 60% of textured ratio and 4.9% of area ratio exhibit the best properties, which could decrease the maximum amplitude by 45.8% at 9000 rpm. In addition, the textured surface with the optimal textured ratio of 60% can reduce the static stiffness and improve the dynamic stiffness. Therefore, partially textured bearings are particularly significant to the stability enhancement of the bearing system, which can lead to the performance and security improvement of the sliding bearing in high-speed applications.

**Keywords** Partial texture · Hydrodynamic bearing · Vibration reduction · Stiffness test

## 1 Introduction

Current research on hydrodynamic bearing has attracted much attention for its potential applications, including but not limited to the spindle of high-speed machine tool, steam turbine, and engine. A key element in these applications is to decrease the clearance, which could be 20–30% lower than that of the ordinary spindle, in order to increase the rigidity and precision of the high-speed spindle. However, the decrease of flow, because of the low clearance, could cause temperature rise, turbulence, and cavitation, which could lower the stability of the hydrodynamic bearing. This prominent problem has limited the speed of dynamic and static bearing. Therefore, structural innovation is needed for the lubrication mode of hydrostatic bearing.

Recent studies have shown that surface texture on the external surface of a spindle or internal surface of a bearing can change the distribution and mobility rule of lubrication oil, which could regulate the thermodynamic lubrication characteristics of hydrostatic bearings, effectively, by modifying the parameters of surface textures. In the study of the influence of surface texture on dynamic lubrication, many researchers work on the theoretical analysis of the surface texture influence on the performances of a journal bearing [1–3]. The results may show that surface texture can improve the load-carrying capacity and reduce the friction coefficient with various types of surface such as rectangle [4], groove [5], trapezoid [6], and concave or convex micro-spherical [7] textures. Xie ZL et al. [8] reveal the micro-interface lubrication regimes of water-lubricated bearing, using fluid dynamic analysis. Velocity vectors and pressure contours are obtained, while micro-interface lubrication mechanisms are established. The surface with micro-cavities shows better load-carrying capacity and coefficient of friction than the smooth surface. Meng FM et al. [9] show that the bearing with dimple groove textures, depending on the size and position of grooves, can decrease the acoustic power levels of the noise. Moreover, compound groove texture can lower the acoustic power level of the journal bearing, more

✉ Xiuqing Hao  
xqhao@nuaa.edu.cn

<sup>1</sup> College of Mechanical & Electrical Engineering, Nanjing University of Aeronautics & Astronautics, Nanjing 210016, China

<sup>2</sup> State Key Laboratory for Manufacturing Systems Engineering, School of Mechanical Engineering, Xi'an Jiaotong University, Xi'an 710054, China

effectively than the simple groove texture can. Teo WJ et al. [10] show the dominance of the geometrical parameters of texture, combining theoretical analysis and actual implementation, establishing the superior textured surface performance in a hydrodynamic regime of lubrication.

Many recent studies show that partial texture produces a better effect than full texture, provided appropriate parameters and placements. Partial texture with optimum diameter, depth, and density can substantially improve the load-carrying capacity of a structure bearing, bringing its performance up to the same level as that of sophisticated bearings [11–14]. Compared to the fully textured bearing, the partially textured journal bearing with the appropriate textured area is favorable at slightly higher speed values [15]. Furthermore, the optimized partial texture has a beneficial effect on the bearing performance, when the journal is misaligning while under working conditions which is contributed to the hydrodynamic lift [16]. Rao TVVLN et al. [17, 18] verify the improvement in load capacity and reduction in friction coefficient, for partially textured bearings, based on an established mathematic model. Tauvqirrahman M et al. [19] proves that the improved hydrodynamic pressure and the load are highlighted due to the boundary slip effect, caused by textured surface of the bearing. The boundary slip effect is mostly observed in partially textured journal bearings. Rahmani R et al. [20] outline an approach to obtain a set of global optimum parameters for partially textured surfaces, which is suitable to use in a variety of applications. The optimum depth for rectangular and triangular textures can enhance load-carrying capacity and reduce friction, while it is 80–85% and 70–75% of the minimum lubricant film thickness, respectively. Tomar AK et al. [21, 22] study the behavior of spherical journal bearing, with different arrangements of micro-textures, using finite element method. The partially textured surface, including dimple texture and groove texture, could enhance the stiffness coefficient, which could improve the stability and decrease the frictional loss more efficiently, compared to the fully textured surface. The aforementioned research works show that partially textured surface can effectively improve the properties of sliding bearings. However, most of the results are analyzed theoretically, using modeling methods. Obviously, detailed tests are needed for the further development of partially textured bearings.

In this paper, in order to verify the excellent performance of the partial texture, the untextured bearing, the fully textured bearing, and the partially textured bearing are all fabricated for experimental purpose. Several groups of tests on different micro-textured surface bearings are carried out, using a hybrid bearing rotor system, to investigate the best parameters of the partial texture, in order to enhance the vibration characteristics and the stability of the bearing rotor system.

## 2 Materials and methods

### 2.1 Materials

The material of sliding bearings used in the test is tin bronze (ZQSn6.5–0.1), which is widely used for sliding bearings in the industry. The water-lubricated sliding bearing has the structure of four chambers without the static pressure chamber. The width, external diameter, and internal diameter are 41.6 mm, 60.012 mm, and 50.023 mm, respectively. Four inlet holes 1 mm in diameter are retained on the outlet grooves. The depth of the outlet grooves is 0.8 mm and the width is 2 mm. The unilateral clearance of the bearing and the spindle is  $30 \pm 1 \mu\text{m}$ . Structure and dimension parameters of sliding bearings are shown in Fig. 1. The bearing capacity and support stiffness are insufficient, because of the absence of a static pressure chamber.

The micro-texture on the sliding bearings is created with a new method called electrochemical micromachining (EMM), which is described in our another published paper in detail [23]. The surface texture obtained by EMM is shown in Fig. 2. The surface morphology of the texture is measured by laser scanning confocal microscopy (Olympus OLS4000, Japan).

### 2.2 Configurations

The test system includes bearing test platform and software detection system. The high-speed spindle, as the major part of the bearing test platform, is supported by two hybrid bearings, which facilitates the disassembly and assembly of the spindle. The bearings are installed in the shell, fixed by bracket on the base of the shock absorber. The back end

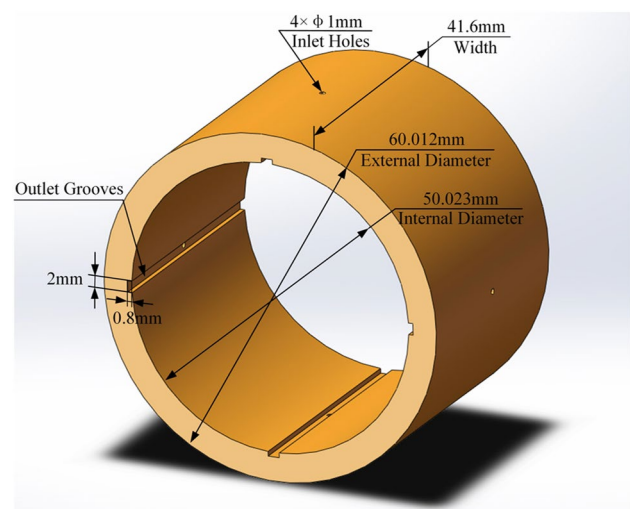


**Fig. 1** Schematic diagram of structure and dimension parameters of sliding bearing

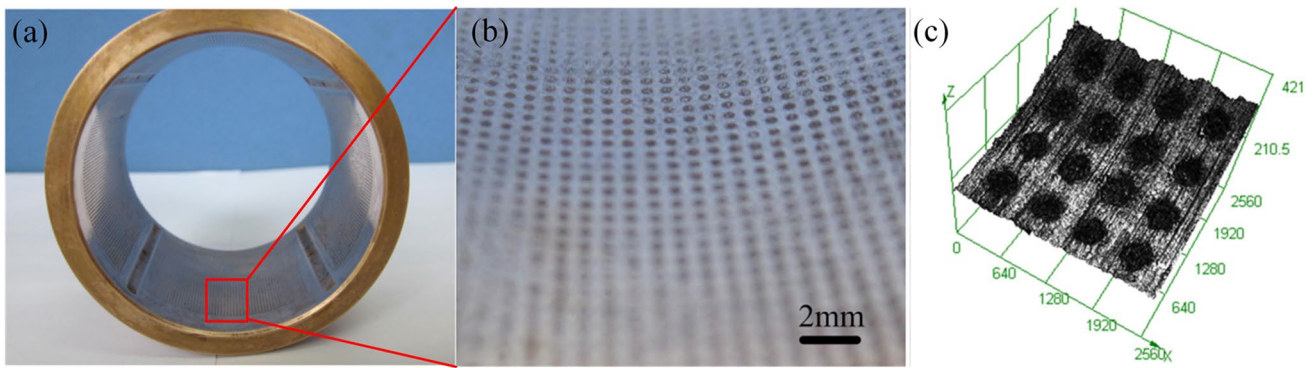


**Fig. 2** **a** The textured bearing fabricated by EMM method. **b** The enlarged photo of the texture on the inner surface of the bearing. **c** Surface morphology of the texture as illustrated by laser scanning confocal microscopy [23]

(driving end) of the shaft is connected to a driving motor, and the front end (working end) is reserved for loading and installing sensors. Motor and rotor are connected with duct tape, to reduce the misalignment between the test shaft and the driving shaft. The speed of the motor is controlled by the frequency converter of the air-bearing motor, which provides different working frequency to the test shaft. The software detection system, aiming to acquire the displacement data rapidly and accurately, is divided into the front part (sensors and transmitters) and the back part (acquisition card and microcomputer). The acquisition system is a NI PXI-1042 case combined with an A/D acquisition card PXI-6255. Two high-precision capacitive displacement sensors (Micro-Epsilon capaNCDT 6100) are used to measure the vibration displacement of the test bearing, in the horizontal and vertical directions. Moreover, LabView is used to code the software for data acquisition with a sampling frequency of 10000 Hz.

Generally, the external load can be changed by the magnitude and rotational speed of the eccentric mass. Hence, the flange plate is fixed on the spindle to change the external load by adjusting the bolts on the plate. In this paper, a bolt of 1.040 g is installed at a radius of 40 mm. At a rotational speed of 2400, 4800, 7200, and 9000 r/min, the calculated eccentric forces at the end of the spindle are 2.628 N, 10.511 N, 23.649 N, and 36.952 N, respectively. In order to ensure the precision of the test result, each experimental condition should be tested at least 6 times. The bearings were installed in water-cooling conditions, in order to improve the accuracy of sleeve positioning and reduce the influence of assembly error.

**2.3 Data processing**

The vibration signal may be disturbed by electromagnetic signal, produced by other devices in the laboratory. Hence, there is much high-frequency noise causing a lot of interference signals that confuse the axis trajectory, as provided

by the displacement sensor. In order to obtain a clear axis trajectory map, to analyze vibration characteristics of the system, the recorded vibration signals need to be filtered.

The signal obtained by the system can be calculated by

$$x(n\Delta t) = A_0 + \sum_{i=1}^N [A_i \sin(\omega_i n\Delta t + \phi_i)] + F_x(n\Delta t) \quad (1)$$

$$y(n\Delta t) = B_0 + \sum_{i=1}^N [B_i \sin(\omega_i n\Delta t + \phi_i)] + F_y(n\Delta t) \quad (2)$$

where  $x$  and  $y$  are the horizontal and vertical displacement signals, respectively;  $A_0$  and  $B_0$  are the horizontal and vertical signal offsets, respectively;  $\omega_i$  is the working frequency;  $A_i$  and  $B_i$  are the horizontal and vertical displacement components, corresponding to the power frequency, respectively; and  $F_x$  and  $F_y$  are the horizontal and vertical white noise components, respectively.

In order to reduce the impact of errors, the trend line of the signal is eliminated, and fast Fourier transformation is used to transform the time domain signal into frequency domain signal. Since the working frequency is related to the vibration caused by rotor, the half frequency, whole frequency, and double frequency are selected to reconstruct the time domain signal. The reconstructed signal can be described by the following formulas, and it can provide the filtered axis trajectory:

$$X(n\Delta t) = A_1 \sin\left(\frac{\omega}{2} n\Delta t + \phi_1\right) + A_2 \sin(\omega n\Delta t + \phi_2) + A_3 \sin(2\omega n\Delta t + \phi_3) \quad (3)$$

$$Y(n\Delta t) = B_1 \sin\left(\frac{\omega}{2} n\Delta t + \phi_1\right) + B_2 \sin(\omega n\Delta t + \phi_2) + B_3 \sin(2\omega n\Delta t + \phi_3) \quad (4)$$

In addition, the maximum vibration displacement of the rotor can be calculated as follows:

$$U_{max} = \sqrt{X^2 + Y^2} \quad (5)$$

### 3 Results and discussion

Partial texture has two important parameters, which are illustrated in Fig. 3. One is the texture rate of texture  $T_p$ , that is, the proportion of the area with texture to the total area. The area ratio can be calculated by the following formula:

$$T_p = \frac{l}{L} \quad (6)$$

where  $l$  is the length of textured surface and  $L$  is the total length of internal surface bearing.

The other parameter is the area ratio of texture  $S_p$ , that is, the degree of dispersion. The area ratio of the partially textured bearing represents the degree of dispersion of the dimples. The area ratio can be calculated by the following formula:

$$S_p = \frac{\pi d^2}{4t^2} \quad (7)$$

where  $S_p$  is the area ratio of the textured bearing,  $d$  is the diameter of the dimples, and  $t$  is the period of the dimples occurrence.

#### 3.1 Effect of textured ratio on stability of the bearing

In this experiment, the depth of the dimples is  $10 \mu\text{m}$ , the diameter of the dimples is  $300 \mu\text{m}$ , and the area ratio of the texture is 4.9%. The textured ratio of three textured bearings  $T_p$ , with serial numbers PM0.3, PM0.6, and PM0.8, is 30%, 60%, and 80%, respectively. Moreover, a full textured bearing named M1 and an untextured bearing named S0 are used for comparison, as demonstrated in Fig. 4. The vibration characteristics of micro-texture on the bearing rotors are studied, considering different area ratio values and speed values of 2400 rpm, 4800 rpm, 7200 rpm, and 9000 rpm, when the water supply pressure is 1.0 MPa. Stability tests were carried out on different samples, while the statistical

results of axis trajectory and amplitude were analyzed as follows.

The amplitude and axis trajectory at the different speed values are shown in Figs. 5 and 6.

It is obvious that the samples with texture exhibit better performance than the sample without texture, which illustrates the role of texture in vibration reduction. In partially textured bearings, there is little difference between the different samples at 2500 rpm and 5000 rpm. However, compared to the non-textured bearing S0, the vibration of the partially textured bearings can be effectively reduced at medium and high rpm values. In this experiment, the texture value of 60% proved optimal. Compared to the sample S0 at 9000 rpm, the relative vibration of sample PM0.6 decreases by 32.3%.

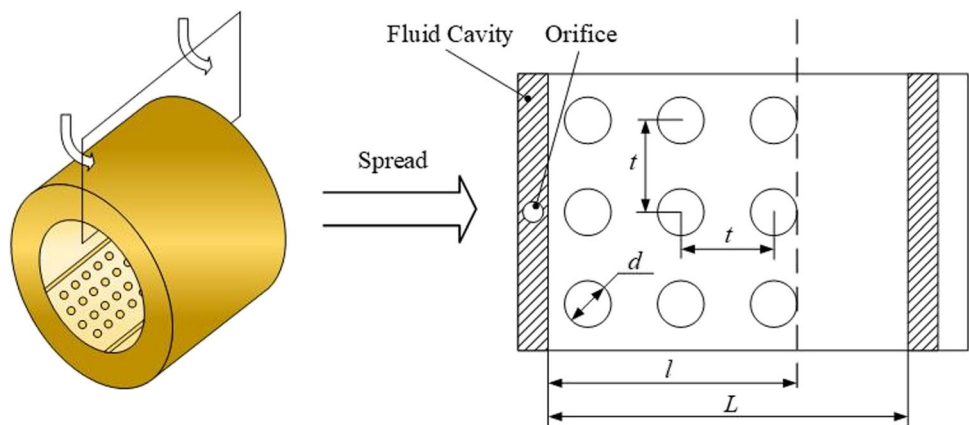
In the experiment, although M1 shows better performance in the low and medium speed range, partially textured bearings produce better effect on the vibration suppression than full textured bearings, especially at a high rotational speed. It can be seen that the relative vibration of PM0.6 in the partial texture bearing is 12.5% lower than that in the full textured bearing M1 at 9000 rpm.

Previous researches show that partial texture has the “collective effect,” when hydrodynamic pressure of lubrication film is generated, so it can reduce the lubrication and friction more effectively than full texture [12, 13, 24, 25]. It is found that the dynamic pressure action of dimples, in the full texture case, produces an individual effect, which can only improve the bearing capacity within limits. Partial textures show an accumulation effect similar to the step or wedge clearance, which can increase the bearing capacity more than the full texture.

#### 3.2 Effect of area ratio on stability of the bearing

In this experiment, the parameters of the dimple remain the same as in the previous section, and the period of the textured bearings is  $600 \mu\text{m}$ ,  $900 \mu\text{m}$ , and  $1200 \mu\text{m}$ , respectively. The corresponding area ratio  $S_p$  of the textured

**Fig. 3** The schematic diagram and spreading diagram of a partially textured bearing





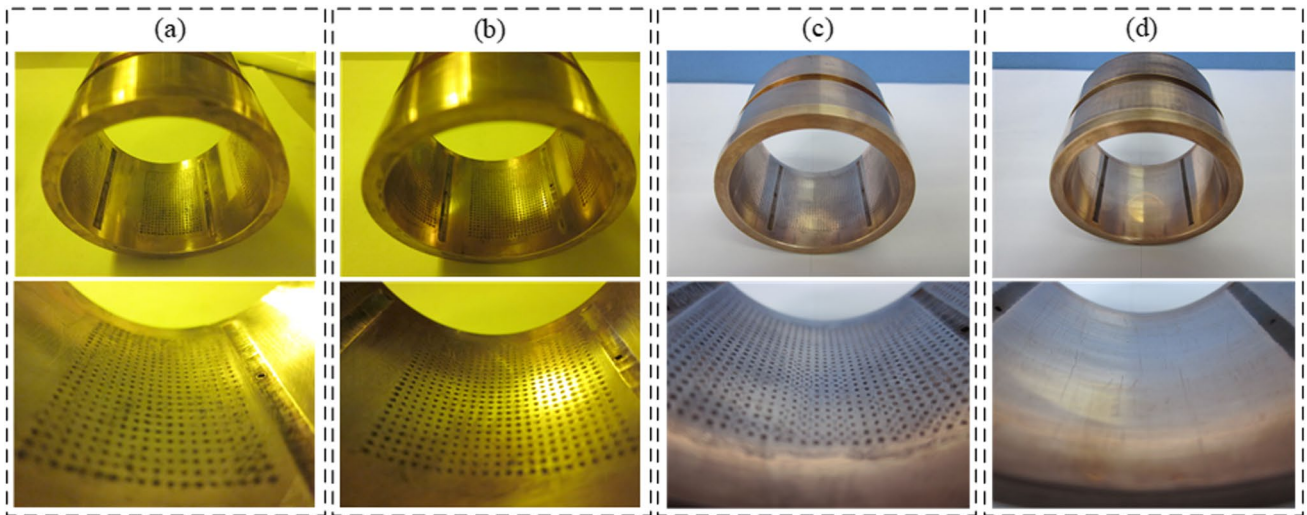


**Fig. 4** Photos of samples with different textured ratio. **a** PM0.6, 60%; **b** PM0.8, 80%; **c** M1, 100%; **d** S0, 100%

bearings PM1, PM2, and PM3 is 19.6%, 8.7%, and 4.9%, respectively. Accordingly, the untextured bearing S0 is used for comparison. The texture rate is selected as 80% in this experiment. The test parameters are the same as those in the previous section. Stability tests were carried out on different samples, while the statistical results of axis trajectory and amplitude were analyzed as follows.

The axis amplitude and trajectory at the different speed values are shown in Figs. 7 and 8. The illustrations show that the axis trajectory remains almost the same across different area ratios at low speed. However, at the speed of 9000 rpm, sample PM3 shows the smallest axis trajectory and PM1 the largest. Obviously, in the case of partial texture, the area ratio of micro-texture has a large influence on the stability of the system, under the condition of medium and low density, but less influence under the condition of high density. This occurs possibly because high density can improve the value of the equivalent film thickness, which can reduce

the stiffness of the system, leading to the decrease of the carrying capacity and stability of the system. However, the partial texture improves the carrying capacity and stiffness of the system. The two sides interact with each other to produce a slight decrease in amplitude. However, the texture has little effect on the equivalent film thickness at medium and low densities, which can improve vibration elimination effectively.

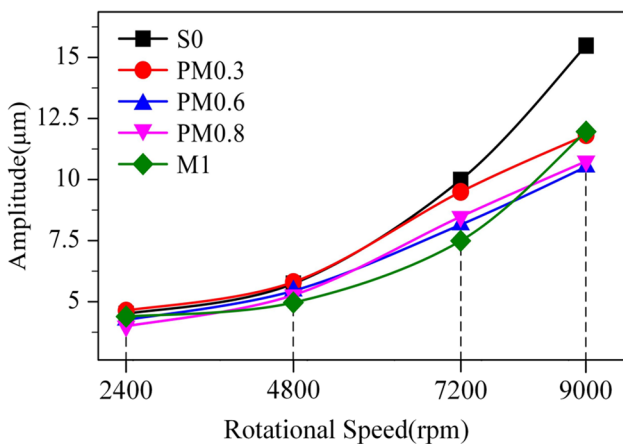


**Fig. 5** The rotor amplitude of bearing rotor systems at different rotational speed values with S0, PM0.3, PM 0.6, PM0.8, and M1 samples

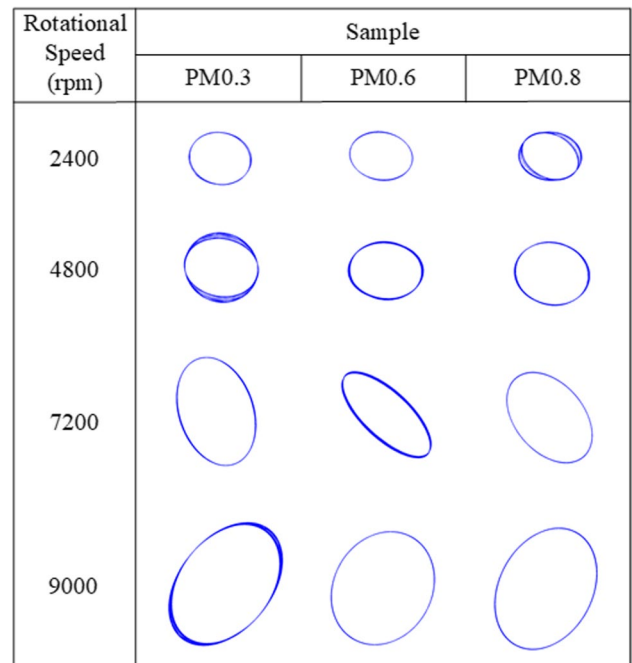


**Fig. 6** The axis trajectory of bearing rotor at 7200 rpm and 9000 rpm under different textured ratios

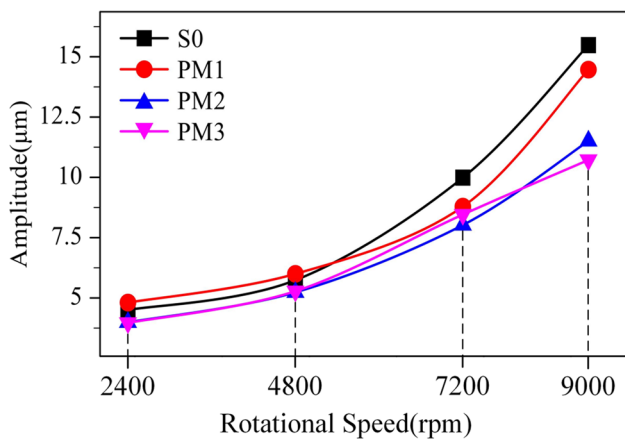


Fig. 7 The amplitude of bearing rotor at different speed values with S0, PM1, PM2, and PM3 samples

### 3.3 Stiffness tests and analysis

#### 3.3.1 Static stiffness analysis

The static stiffness of a bearing system refers to the ratio of load and displacement along a certain loading direction when the spindle is in static suspension state. When the spindle is stationary, the static stiffness is mainly related to the structural geometric parameters, working conditions, and loading direction of the bearing. In the static stiffness test, the oil supply pressure values are 1, 1.5, 2, 2.5, and 3 MPa. The disk weights of the test are 1.35, 2.37, and 3.39 kg,

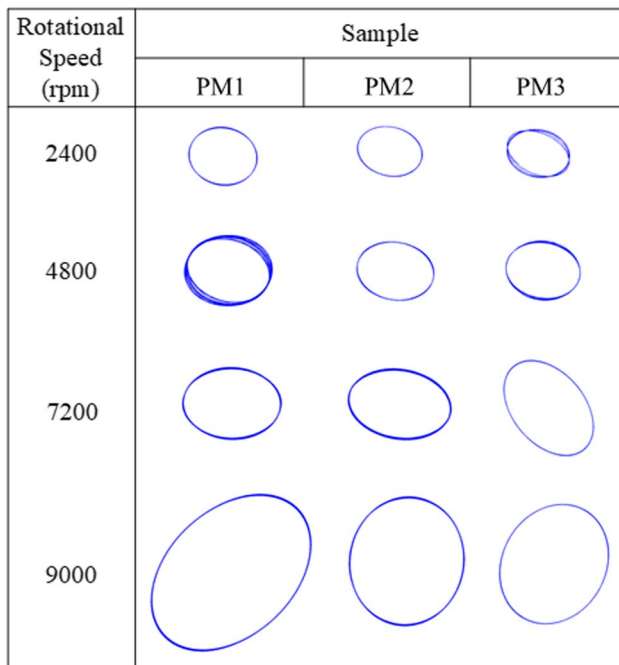


Fig. 8 The axis trajectory of bearing rotor at different speed values under different area ratios

which means the loading forces on the front bearing are 23.05 N, 40.47 N, and 57.88 N, along the vertical loading direction, respectively.

The test results of different partially textured bearing systems, when the loading force is 23.05 N, are shown in Fig. 9. It can be seen that the static stiffness increases as the water pressure rises, whereas the growth rate becomes slower when the water pressure reaches higher than 2 MPa. The textured surface could reduce the static stiffness of the system under constant loading force and water pressure. Moreover, the greater the textured ratio, the faster the static stiffness becomes lower. Due to the increase of oil supply pressure, the lubricant in the bearing spreads out faster within the clearance space, which is conducive to the formation of lubricating oil film. Because of the dimples on the surface, the equivalent bearing clearance and the film thickness appear increased. Higher area ratio means higher film thickness, so the static stiffness is lower.

When the water supply pressure is 3 MPa and the loading forces are 23.05 N, 40.47 N, and 57.88 N, the respective rotor static stiffness values of partially textured bearings are listed in Table 1. The static stiffness of the spindle initially increases, followed by a decrease as the loading force increases. This occurs mainly due to the increasing displacement of the spindle along the loading direction, when the loading force rises. The degree of eccentricity could deviate from the condition of the linear hypothesis of small eccentricity in the calculation of the static stiffness of the spindle.

#### 3.3.2 Dynamic stiffness analysis

Dynamic stiffness of a bearing rotor system, that is, the comprehensive stiffness of rotation, refers to the ratio of load and corresponding displacement along a certain loading direction, under a constant spindle speed. At high spindle rotational speed values, the bearing works within the comprehensive action of dynamic and static pressure. In addition to the structural parameters and loading direction of the

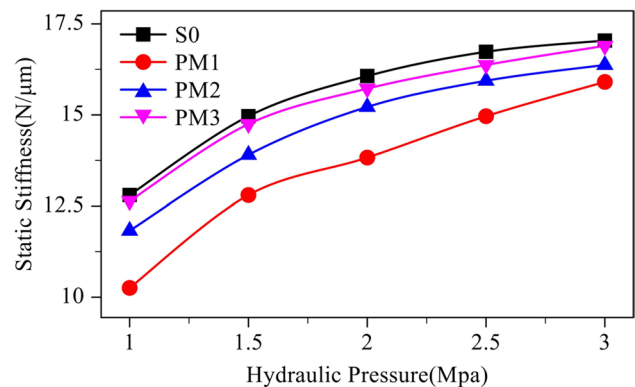


Fig. 9 The relationship between hydraulic pressure and static stiffness of S0, PM1, PM2, and PM3 samples

**Table 1** The rotor static stiffness of bearing samples

Loading force (N)	S0	M1	PM0.3	PM0.6	PM0.8
23.05	17.04	16.16	15.81	16.05	16.16
40.47	24.59	23.69	21.67	24.17	23.69
57.88	14.14	13.45	11.70	13.02	13.45

bearing, the influence of surface morphology on the dynamic pressure of the bearing is also highlighted. In the dynamic stiffness test, the water supply pressure is 1 MPa, the loading force is 12.51 N, and the frequency is 40–150 Hz, adjusted to increase by 10 Hz at each iteration (rotational speed = frequency multiplied by 60), while the loading direction is vertical. In order to compare the effects of non-textured, full textured, and partial textured samples on the dynamic stiffness, non-textured samples S0, full textured samples M1, and samples with three different textural ratios are selected for statistical purpose. The results are shown in Fig. 10.

Obviously, at low speed, the dynamic stiffness of the different surface system shows little difference. However, the dynamic stiffness of all three textured samples is higher than the non-textured surface S0, when the speed reaches the medium value level of 4200 rpm. At a rotating speed higher than 6000 rpm, the dynamic stiffness of all partially textured samples is higher than that of the fully textured surface, whereas the optimal textural ratio proves to be 60% (PM0.6). At 9000 rpm, compared to S0 and M1, the increase in dynamic stiffness of the sample PM0.6 is 22.1% and 10.3%, respectively.

At low velocity, the bearing with full texture or high textured ratio shows better performance, because static pressure is dominant compared to dynamic pressure. As the rotational speed rises, dynamic pressure has a growing influence on the system. Moreover, the existence of dimples is equivalent to higher film thickness. There is a competitive relationship between the decrease of bearing capacity, caused by the increase of film thickness and the increase of dynamic pressure caused by the micro-texture. Therefore, compared to the fully textured surface, the dynamic stiffness and stability of partial texture bearing rotor system enhance at high rotational speed, which is also consistent with axis trajectory test results. In this experiment, the optimal textured ratio is 60%.

### 4 Conclusions

In this work, considering smooth surface and fully textured surface, the outstanding performance of sliding bearings with partially textured surface is verified by testing on the bearing test platform. Based on the experimental results and theoretical analysis, conclusions can be summarized as follows:

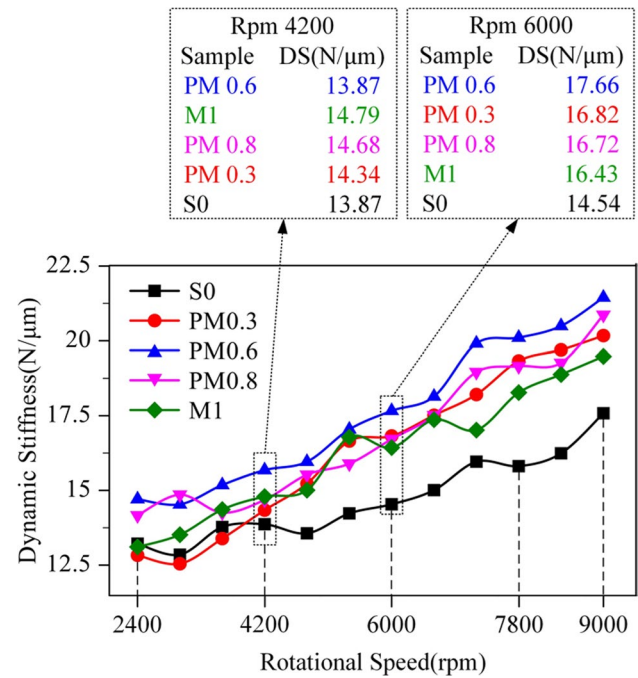


**Fig. 10** Dynamic stiffness at different rotational speed values with S0, PM0.3, PM0.6, PM0.8, and M1 samples and comparison results for dynamic stiffness at 4200 and 6000 rpm

- (1) The two important parameters, textured ratio and area ratio, have enormous influence on the properties of the partially textured bearing. The appropriate partial texture can play a greater role, at high-speed operation, where it shows better vibration suppression effect than the full texture. The optimal textured ratio  $T_p$  and area ratio  $S_p$  prove to be 60% and 4.9% respectively, significantly lowering the maximum amplitude by 45.8% at 9000 rpm.
- (2) Partial texture with appropriate parameter could reduce the static stiffness and improve the dynamic stiffness of the bearing system. In partially textured samples, the area ratio appears to have little effect to static stiffness, whereas 60% is considered as the optimal textured ratio. Regarding dynamic stiffness, the maximum increment is 22.1%.
- (3) The experimental results show that the reasonable choice of texture can significantly reduce the vibration amplitude of the bearing rotor system enhance the stability of the system, and increase the stiffness of the lubrication film.

Future work will move forward to consider the actual structure of the bearing and the pressure distribution during the working process, combined with surface/interface physics, physical and chemical properties of materials, and other basic theories especially at high-speed and ultra-high-speed values. Further theoretical and experimental research is

needed to perfect the layout of the texture zone on the inner surface of the bearing. In addition, an appropriate method should be established to measure the friction force on the surface of the bearing, during operation, directly or indirectly. These studies are expected to further improve bearing performance, thus expanding the application spectrum into microfluidics, aviation, navigation, and other domains.

**Funding** The authors greatly acknowledge the financial support from the National Natural Science Foundation of China (51875285), the Natural Science Foundation of Jiangsu Province (BK20190066), the College Young Teachers Fund of the Fok Ying Tung Education Foundation (20193218210002), the Fundamental Research Funds for the Central Universities (NE2020005), and the State Key Laboratory of Mechanical System and Vibration (MSV202008).

**Data availability** Available.

**Code availability** Not applicable.

## Declarations

**Ethics approval** Approval.

**Consent to participate** Approval.

**Consent for publication** Approval.

**Conflict of interest** The authors declare no competing interests.

## References

- Kango S, Singh D, Sharma RK (2012) Numerical investigation on the influence of surface texture on the performance of hydrodynamic journal bearing. *Meccanica* 47(2):469–482
- Wang SH, Wu XY, Zheng JH (2011) Influence of surface texture on lubrication performance of hydrodynamic journal bearing. *Appl Mech Mater* 120:426–431
- Meng FM, Shu RH, Chen L (2020) Influences of operation parameters on noise of journal bearing with compound texture considering lubricant thermal effect. *Proceedings of the Institution of Mechanical Engineers, Part J: Journal of Engineering Tribology* 234(7):991–1006
- Yu RF, Chen W, Li P (2016) The analysis of elasto-hydrodynamic lubrication in the textured journal bearing. *Proceedings of the Institution of Mechanical Engineers, Part J: Journal of Engineering Tribology* 230(10):1197–1208
- Feng HH, Peng LP (2018) Numerical analysis of water-lubricated thrust bearing with groove texture considering turbulence and cavitation. *Industrial Lubrication and Tribology* 70(6):1127–1136
- Rao TVVLN, Rani AMA, Nagarajan T, Hashim FM (2013) Load capacity of partially textured journal bearing with trapezoidal recess. *Appl Mech Mater* 315:830–834
- Wang J, Zhang JH, Lin JW, Ma L (2018) Study on lubrication performance of journal bearing with multiple texture distributions. *Appl Sci* 8(2):244
- Xie ZL, Zhang Y, Zhou JZ, Zhu WD (2021) Theoretical and experimental research on the micro interface lubrication regime of water lubricated bearing. *Mechanical Systems and Signal Processing* 151: 107422.
- Meng FM, Zhang W (2018) Effects of compound groove texture on noise of journal bearing. *Journal of Tribology* 140(3): 031703.
- Teo WJ, Dolatabadi N, Rahmani R, Morris N, Rahnejat H (2018) Combined analytical and experimental evaluation of frictional performance of lubricated untextured and partially textured sliders. *Lubricants* 6(4):88–88
- Etsion I, Halperin G (2002) A laser surface textured hydrostatic mechanical seal. *Tribol Trans* 45(3):430–434
- Etsion I (2004) Improving tribological performance of mechanical components by laser surface texturing. *Tribol Lett* 17(4):733–737
- Brizmer V, Kligerman Y, Etsion I (2003) A laser surface textured parallel thrust bearing. *Tribol Trans* 46(3):397–403
- Etsion I, Burstein L (2008) A model for mechanical seals with regular microsurface structure. *Taylor & Francis Group* 39(3):677–683
- Tala-Ighil N, Fillon M (2017) Performance evolution of fully and partially textured hydrodynamic journal bearings lubricated with two lubricants. *IOP Conference Series: Materials Science and Engineering* 174(1): 012032.
- Song XT, Wu W (2020) The effect of journal misalignment on the lubrication performance of partially textured journal bearing with elastic deformation. *Journal of Physics: Conference Series* 1549(3): 032070.
- Rao TVVLN, Rani AMA, Nagarajan T, Hashim FM (2012) Analysis of slider and journal bearing using partially textured slip surface. *Tribol Int* 56:121–128
- Rao TVVLN, Rani AMA, Nagarajan T, Hashim FM (2014) Analysis of couple stress fluid lubricated partially textured slip slider and journal bearing using narrow groove theory. *Tribol Int* 69:1–9
- Tauviqirrahman M, MuchammadJamari ARA (2018) Influence of boundary slip layout on the hydrodynamic performance of partially textured journal bearing by CFD method. *MATEC Web of Conferences* 204:04008
- Rahmani R, Rahnejat H (2018) Enhanced performance of optimised partially textured load bearing surfaces. *Tribol Int* 117:272–282
- Tomar AK, Sharma SC (2020) An investigation into surface texture effect on hole-entry hybrid spherical journal bearing performance. *Tribology International* 151:106417
- Tomar AK, Sharma SC (2020) A study of hole entry grooved surface hybrid spherical journal bearing operating with electrorheological lubricant. *Journal of Tribology* 142(11):111802
- Hao XQ, Sun HL, Wang L, Ali Q, Li L, He N (2020) Fabrication of micro-texture on cylindrical inner surface and its effect on the stability of hybrid bearing. *Int J Adv Manuf Technol* 109:1671–1680
- Kligerman Y, Etsion I, Shinkarenko A (2005) Improving tribological performance of piston rings by partial surface texturing. *Transactions of the ASME Journal of Tribology* 127(3):632–638
- Ryk G, Etsion I (2006) Testing piston rings with partial laser surface texturing for friction reduction. *Wear* 261(7–8):792–796

**Publisher's note** Springer Nature remains neutral with regard to jurisdictional claims in published maps and institutional affiliations.